Electrolyte-Gated Colloidal Nanoplatelets-Based Phototransistor and Its Use for Bicolor Detection

Emmanuel Lhuillier, Adrien Robin, Sandrine Ithurria, Herve Aubin, Benoit Dubertret

Electrolyte gated colloidal nanoplatelets based phototransistor and its use for bicolor detection

E. Lhuillier[1], A. Robin[1,2], S. Ithurria[2], H. Aubin[2], B. Dubertret[2*]

[1]Solarwell, 10 rue Vauquelin, Paris, France

[2]LPEM, ESPCI 10 rue Vauquelin, Paris, France

Abstract: Colloidal nanoparticles are appealing candidates for low cost optoelectronic applications since they can combine the advantages of both organic materials -such as their easy processing- and the excellent performances of inorganic systems. Among colloidal nanoparticles, 2D shaped nanoparticles have become particularly popular since the rise of graphene. Here we report the use of 2D colloidal nanoplatelets for photodetection. We show that the nanoplatelets photoresponse can be enhanced by two to three orders of magnitude when they are incorporated in an all solid electrolyte gated phototransistor. We extend this technique to build the first colloidal quantum dot based bicolor detector, with a response switchable between the visible and near-IR.

Keyword : Nanosheets, photodetector, transistor, electrolyte, bicolor detector.

INTRODUCTION

Photodetection devices based on colloidal quantum dot (CQD), have mainly been developed for solar cells applications[1], although photodetectors[2] from UV[3] to mid IR[4] have also been reported. The responsivity of a photodetector remains strongly determined by the product of the carrier mobility and the minority carrier lifetime[5, 6]. Optimal photodetectors require both large mobilities as well as large densities of photogenerated charge carriers. The carriers mobility of films formed of colloidal materials has increased substantially lately[7, 8] but strategies geared toward enhanced photo-generated charge carriers densities remain necessary. Enhanced carrier densities can be obtained either using a photoactivation (multi-exciton generation[9, 10]) or an electrical process. Within the latter approach, two strategies are worth mentioning: carrier avalanche in a high electric field region, and phototransistors,[11] which take advantage of the non-linearity of the current with the carrier density. In this paper we propose to develop phototransistors while using colloidal material as the active layer.

CQD-based phototransistors[12, 13] have remained mostly under-developed since they suffer from the fact that the nanoparticles' film thickness, and thus the device absorption, need to remain small so that the charge carriers modulation is obtained on the whole film thickness when the gate voltage is turned on. In other words, the back gated field effect transistor[14] cannot combine both a strong absorption and a large current/responsivity modulation. Recently, however a report has described colloidal quantum dot-based electrochemical transistors[15] (ET) with exceptional performance (on/off ratio as high as 10^9 and subthreshold slope as low as 80mV/decade). Such ET are particularly interesting from a photodetection point of view since the nanoparticles charging can be achieved even in thick films. The goal of this paper is to demonstrate an increased responsivity for electrolyte gated films of colloidal nanomaterials. In addition, we demonstrate a device for multicolor detection, a step which has not been reported yet using CQD, but that is important if CQD based optoelectronic[16] devices want to compete ultimately with existing technologies.

FROM PHOTODETECTOR TOWARD PHOTOTRANSISTOR

In this work, we use mainly colloidal nanoplatelets (NPLs)[17] instead of CQDs, because they have been shown to provide electrolyte gated FET with higher performances than when spherical CQDs are used[15]. Among colloidal materials, 2D materials have confinement in only one dimension. If atomic control is achieved in this direction, extremely narrow excitonic features can be achieved[17, 18]. So far most of the work on this material has been focused on their synthesis or optical properties, with just few examples dedicated to their integration in devices[15, 19]. In this work, we have synthesized core/shell[20] CdSe/CdS nanoplatelets with 3.5 monolayers (ML) of CdS. These NPLs show a first excitonic transition at 630nm, with a photoluminescence linewidth around 20nm, see Figure 1 (a) and supplementary information for details about the synthesis. The NPLs are typically 4nm thick, with lateral extension of 10x20nm (Figure 1 a)).

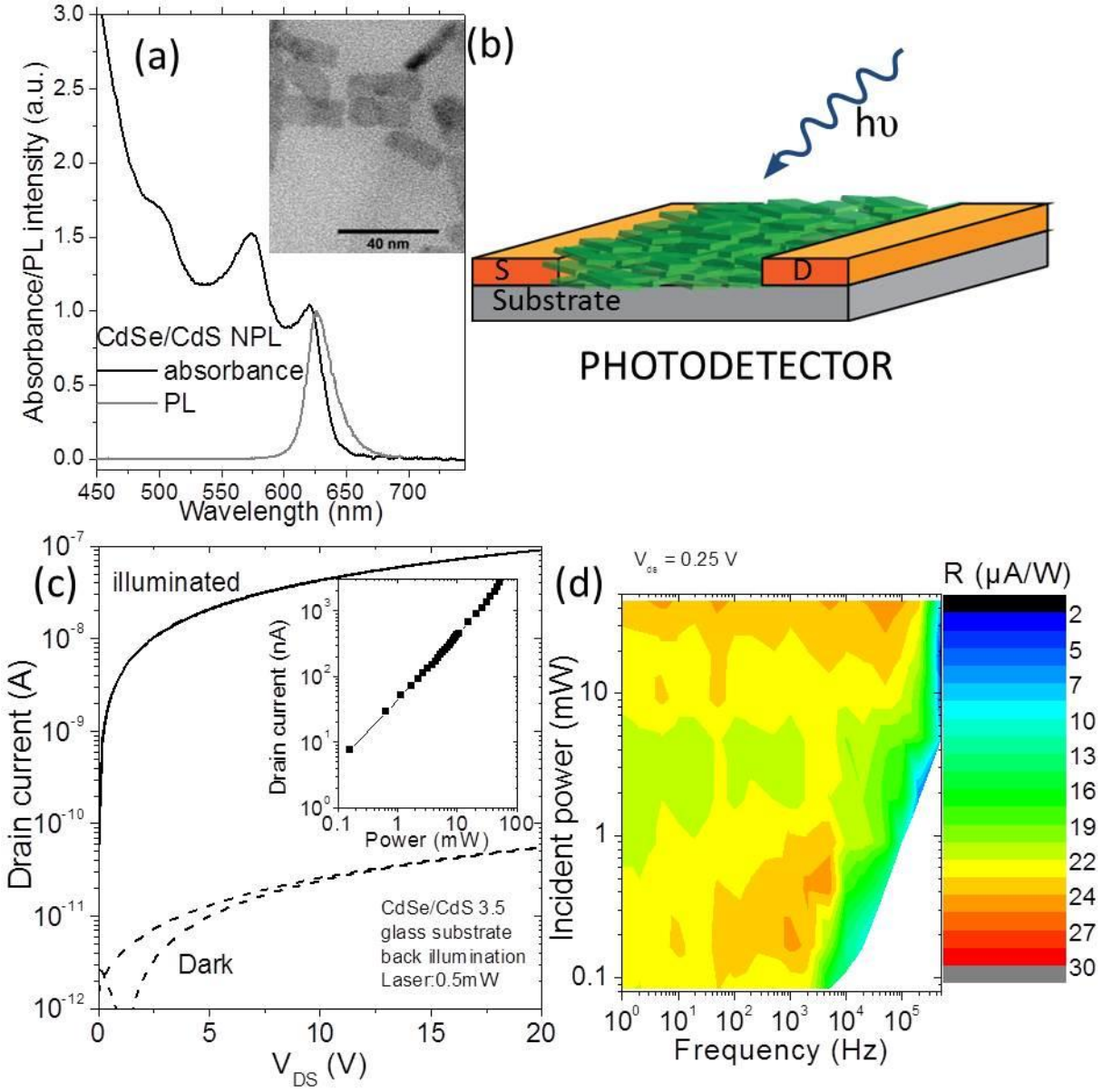

Figure 1 (a) absorption and photoluminescence spectrum of a solution of CdSe/CdS NPLs. The inset is a transmission electron microscopy image of the CdSe/CdS NPLs. (b) Scheme of a photodetector. S and D stand respectively for source and drain. (c) Current as a function of the applied bias in a film of CdSe/CdS NPLs in the dark and under illumination (λ=405nm - P≈17mW.cm^{-2}). The inset is the dependence of the current as a function of the incident light power (d) Responsivity for a film of the same material as a function of the light modulation frequency and power. The drain source bias is set at 0.25V.

After the synthesis, we perform a ligand exchange[21] in solution with S^{2-}. This exchange provides stronger electronic coupling between the particles when they are assembled in films, so that mobility μ in the range 10^{-2}-1 $cm^2V^{-1}s^{-1}$ are obtained, depending on the annealing temperature. A scheme of the photodetector is shown on Figure 1 (b). Due to the wide band gap of the material (band edge energy E_G≈2eV), the number of thermally activated carriers n_{dark} remains low, since $n_{dark} \propto \exp\left(-E_G / 2k_bT\right)$, where k_bT is the thermal energy. Under illumination, the conductivity strongly increases by several orders of magnitude; see Figure 1 (c). The change of conductance $\Delta\sigma$ upon illumination can easily be related to the carrier density generated optically[22], Δn_{op}, using the relation $\Delta n_{op} \propto \Delta s / e\mu$ (e is the proton charge), from which we can obtain an upper value $\Delta n_{op} \approx 2.10^{14} cm^{-3}$ corresponding to 1 optically pumped carrier per 2000 NPL (we have assumed that μ≈10^{-2} $cm^2V^{-1}s^{-1}$, and that the NPLs are randomly packed with a density of 0.64). This low density of optically activated carriers seems consistent with the short photocarrier lifetime (τ) measured experimentally. Indeed, the response of the system is rather fast and was above the measurement capacities of our setup (f_{3dB}>100kHz or τ<10μs), see Figure 1 (d). The price of this

fast time response is the fact that the absolute value of the responsivity remains quite low (typically tens of µA/W). These limited values for the responsivity are consistent with older value reported when CdSe spherical CQDs[23] are used. We also note that the responsivity of the material is fairly independent of the incident photon flux (i.e. current rises linearly with the photon flux from 10 to 2000 mW cm^{-2}), see the inset of Figure 1 (c). This means that no significant band bending occurs for this range of photo-induced charges.

To improve the detection performances of NPLs based photodetector we now explore the possibility to use films of NPLs to detect light when used in a transistor geometry. A film of CdSe/CdS NPLs can be gated with a polymer electrolyte (see Figure 2 (a) for a scheme of the device) leading to n-type carrier conduction. We have demonstrated that NPLs based electrolyte transistors can have ON/OFF ratio close to 10^9 (Fig. 2b). In a previous paper[15] we have demonstrated that this strategy enables the bulk doping of the whole film thickness with the ions from the electrolyte, even for micron thick films. The possibility to charge thick NPLs films is interesting because with an absorption coefficient typically around $2x10^3 cm^{-1}$ at the first exciton (see figure S2), several microns of NPLs are necessary to absorb light efficiently. ET presents large current modulation under a limited change of the applied gate bias. Our strategy is to bring the gate bias close to the turn-on bias and then take advantage of the photogenerated excess of charge to induce a strong (photo)-current modulation (fig. 2b).

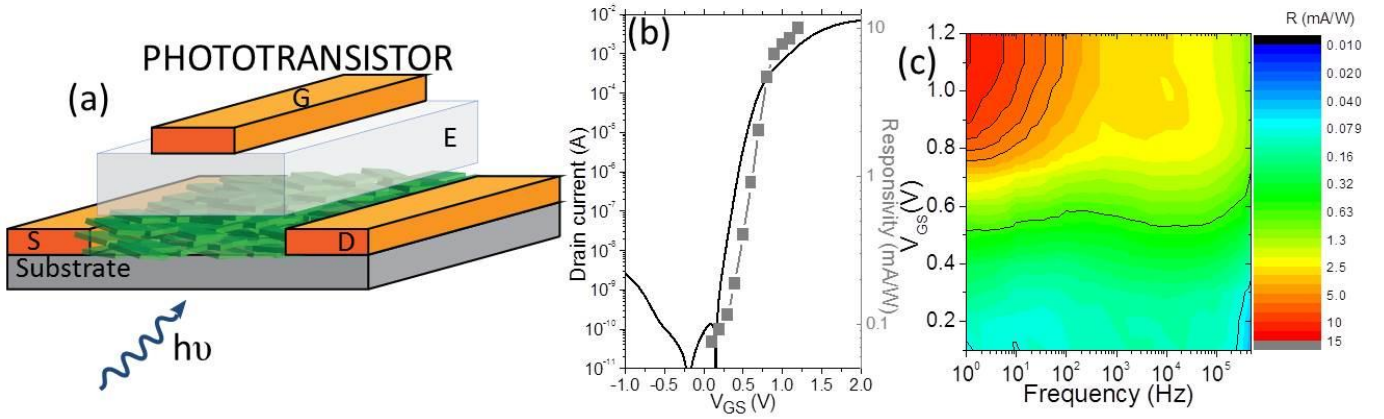

Figure 2 (a) Scheme of a photodetector. S D and stand respectively for source, drain and gate while is E for electrolyte. (b) drain current in the dark (V_{DS}=0.5V) and responsivity at 10Hz (V_{DS}=1V) as a function of gate bias for a CdSe/CdS NPL film. (c) Map of the responsivity of a CdSe/CdS NPL film as a function of light frequency modulation and gate bias. The incident light power is 20mW and the drain-source bias is set equal to 1V.

We observe that when the gate bias rises from 0V (where the system is just photoconductive) to 1V (where charges are injected) the responsivity rises by a factor of 100 to 1000 depending on the frequency, see Figure 2 (c). The phototransistor typically reaches values of tens of $mA.W^{-1}$ (compared to tens of µA W^{-1} in the photoconductive mode). It is also worth noticing that while in a photoconductive mode, the photoresponse barely dependends on the frequency (Figure 1 (d)), we observe a much stronger frequency dependence of the response in the phototransistor mode, see the upper part of Figure 2 (c).

We now turn to a description of the charge carriers recombination mechanisms in our phototransistor. The gate bias voltage dependence presented in Fig. 2b can be schematically presented with three regimes that are described on Figure 3. When no gate bias is applied, the system remains poorly conducting. Photocarriers can be generated by light absorption, but they are rapidly trapped by empty states near the conduction band (surface traps, see Figure 3 (d). In this regime, the gain remains low and the dark current rises compared to the pure photoconductive mode, due to leakage current through the gate. No photodetection gain is obtained.

When a gate bias is applied, the Fermi level starts to shift toward the conduction band and the traps are filled. At the threshold voltage, most of the localized trap states are filled and newly thermally or photogenerated carriers drift under electric field in the conduction band, see Figure 3 (a) and (e). The minority carrier lifetime is enhanced compared to the lower gate bias regime, resulting in a higher gain and an improved responsivity.

At even higher gate bias, the Fermi level reaches the conduction band and carriers are directly injected into the conduction band, which results in a bleach of the absorption of the first exciton[15, 24], see Figure 3 (b) and (f). The cross section and the responsivity are consequently affected. From a pure transport point of view, the subthreshold slope is generally also increased. Consequently this regime is more adapted for electrochromism applications rather than photodetection.

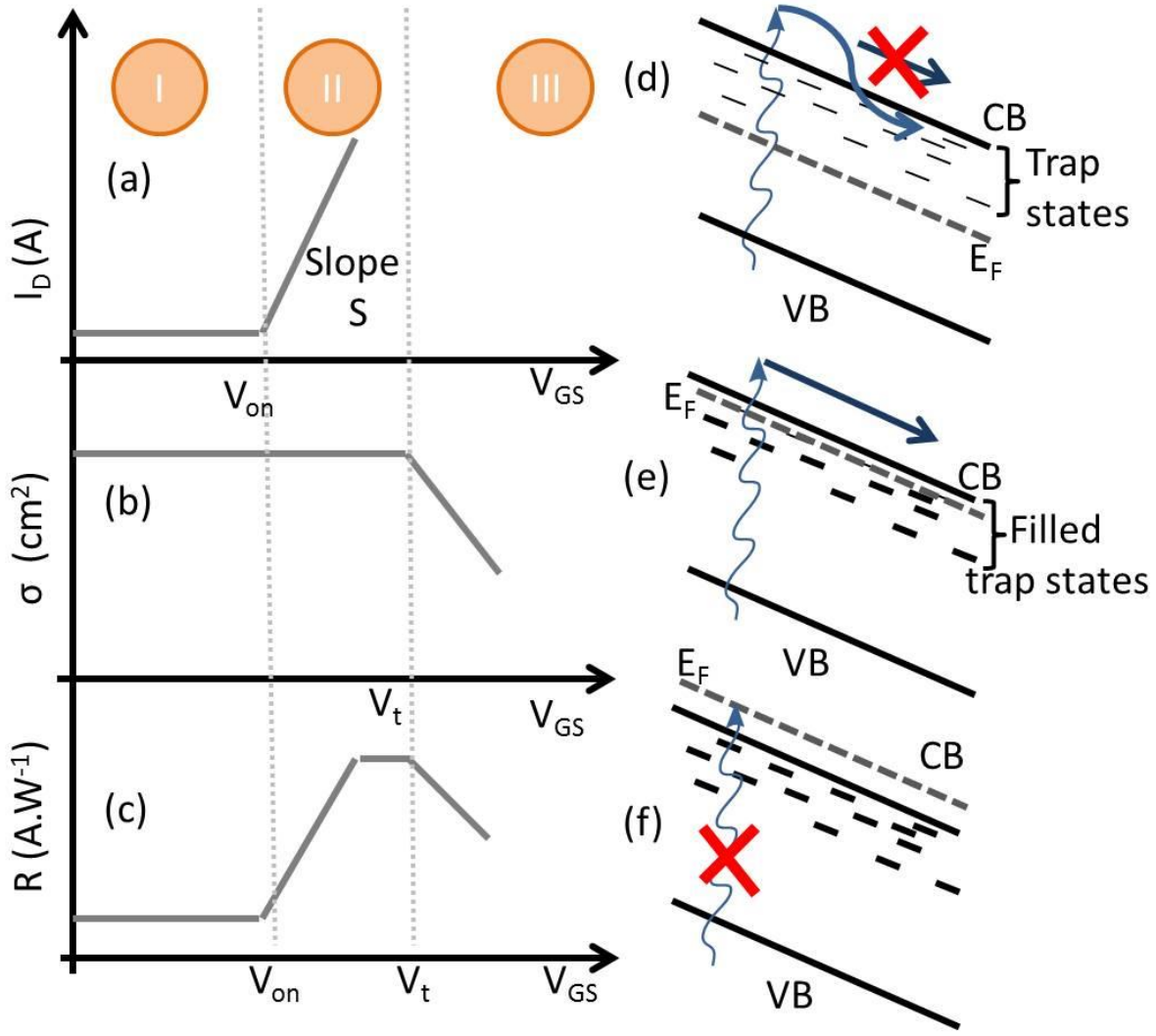

Figure 3 (a) Scheme of the drain current as a function of the gate source bias for a CdSe/CdS nanosheets based ET. (b) Scheme of the absorption cross section as a function of the gate source bias for a CdSe/CdS nanosheets based ET. (c) Scheme of the responsivity as a function of the gate source bias for a CdSe/CdS nanosheets based ET. (d) (e) and (f) are scheme of the band diagram at three different levels of the gate bias.

In a field effect transistor the current can be written[25]

$I(V_{DS},V_{GS}) = I_{dark}(V_{DS},V_{GS}=0)\left[1+10^{\frac{V_{GS}-Vt}{S}}\right]$, where *S* is the subthreshold slope and V_t the threshold voltage.

Under illumination, an excess of charges, Δn, is photogenerated and the effective bias driving the transistor becomes $V_{GS}+\frac{\Delta n}{C_G}$, where C_G is the gate capacitance. Under illumination, the current becomes:

$$I(V_{DS},V_{GS}) = I_{dark}(V_{DS},V_{GS}=0)\left[1+10^{\frac{V_{GS}+\frac{\Delta n}{C_G}-Vt}{S}}\right] + \Delta n \cdot \mu \cdot E \quad (1)$$

with *E* the applied electric field over drain-source and μ the carrier mobility. The excess of charge is given by the expression $\Delta n = \frac{eN\sigma\tau\phi}{E_{ph}}$ where *e* the proton charge, N the total number of NPL absorbing, σ the cross section of

the particle, τ the minority carrier lifetime into the film, ϕ the power flux per unit area and E_{ph} the energy of the incident photon.

The last term of equation (1) corresponds to the photocurrent in the photoconductive mode, but the enhanced photoresponse is related to the term $10^{\frac{V_{GS}+\frac{\Delta n}{C_G}-Vt}{S}}$. Finally the change in the responsivity (*R*) compared to the regular photodetector (R_{det}) is given by

$$\frac{R-R_{\det}}{R_{\det}} = I_{dark}(V_{DS}, V_{GS}=0V)\cdot 10^{\frac{V_{GS}-V_t}{S}} \frac{10^{\frac{\Delta n}{C_G S}}}{\Delta n\cdot\mu\cdot E_{\det}}$$
$$= \underbrace{I_{dark}(V_{DS}, V_{GS}=0V)\cdot 10^{\frac{V_{GS}-V_t}{S}}}_{\text{Dark current enhancement}} \underbrace{\frac{10^{\frac{eN\sigma\tau\phi}{E_{ph}C_G S}}}{\Delta n\cdot\mu\cdot E}}_{\text{Photoresponse enhancement}} \quad (2)$$

There are clearly two components in equation (2). The left part is related to the enhancement of the dark current by the gate. The absolute value of the responsivity is indeed increased but the signal to noise ratio (detectivity) is not. The right term is the most interesting since it corresponds to a responsivity enhancement factor which comes without an increase of the dark current. The response increase is predicted to be higher for long photocarrier lifetime which is consistent with the observed responsivity measurement (Figure 2 (c)) where low frequency (*i.e.* long photocarrier lifetime) are more enhanced than the fast component.

From equation (2), we can define a subthreshold slope for the response S_R equal to $\frac{V_{GS}}{S_R} = \frac{eN\sigma\tau(V_G)\phi}{E_{ph}C_G S}$. We typically obtained value of 0.3V/decade at 10Hz. ideally we would like to operate the phototransistor in a range of flux for which $S_R<S$, in order to enhance both responsivity and detectivity. This means that the full potential of the phototransistor will be exploited either at low frequency or under high flux.

Finally we discuss the possibility of using the electrolyte gating as a switch to build a bicolor detector. To build such a detector with a limited overlap of the photoresponse, two materials with different bandgaps are necessary. For an equal inter-particle coupling (*i.e.* same carrier mobility), the material with the reddest response (narrower band gap) is generally more conductive due to the higher thermally activated carrier density. Since the output signal is a current we want to use the electrolyte gating as a strategy to tune the carrier density of the wide band gap material above the one of narrow band gap material. Here we want to use the electrolyte as a tool to tune the relative quantum yield of the two materials to build the bicolor detector.

To realize this device, a possible strategy is to combine two unipolar materials (one p, one n) with different optical features. While the CdSe/CdS NPL constitute the n-layer, we tried CdTe NPL or the organic conducting polymer P3HT as the p-layer. We made ambipolar transistors with strong on/off ratios, see supplementary information figure S4, but the p layer was non photo-responsive in the case of P3HT and was suffering from a lack of stability in the case of CdTe. The strategy we chose next was to combine HgTe QD[4] (see sup info) with CdSe/CdS NPL. The absorption spectra of the two materials are plotted on Figure 4 (c). The HgTe QD have the advantage of being both optically active up to the mid-IR[26] and sufficiently conductive[27] (due to large number of thermally activated carriers at room temperature[28]) even without charging.

A scheme of the device is shown on Figure 4 (a). The HgTe QDs and CdSe/CdS NPLs are electrically connected in parallel. Under low gate bias, the CdSe/CdS NPLs are strongly insulating and the transport is dominated by the conduction in the HgTe QDs. Since the HgTe film is not gated, there is no current modulation while tuning the gate bias, see Figure 4 (b). In this regime we observe a photoresponse under light illumination at both 405nm and 980nm, Figure 4 (d). The responsivity of the HgTe layer is typically at 170µA.W^{-1} at 980nm and 0.8mA.W^{-1} at 405nm. The associated external quantum efficiency (EQE) is given by $EQE = \frac{hv.R}{e}$ and is 0.02% at 980nm and 0.25% at 405nm.

When the gate bias is increased, above the turn on voltage of the CdSe/CdS layer, typically around 0.8V, the conductance of the CdSe/CdS NPL rises and eventually exceeds that of the uncharged HgTe QD, see Figure 4 (b). The response under near IR illumination disappears and the response in the blue rises significantly see Figure 4 (e) and (f). The EQE is now 1.5% at 405nm and 1.2V gate bias, while it vanished below the setup resolution at 980nm. To

summarize, under low gate bias the system detects light from UV to mid-IR, while at high gate bias the system is only sensitive to visible light. This device is so far the first bicolor colloidal nanoparticle based photodetector.

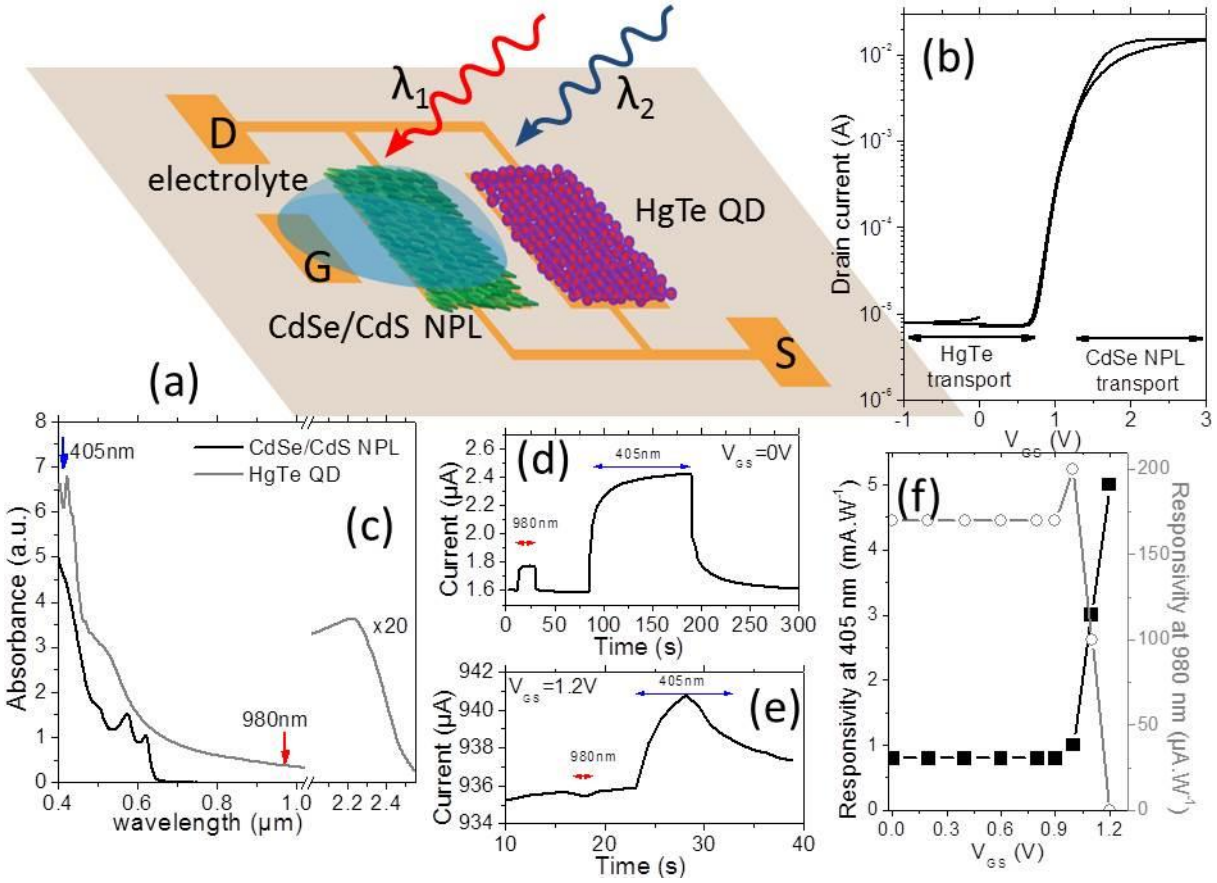

Figure 4 (a) Scheme of the bicolor device. (b) Drain current vs gate bias charateristic of the bicolor device. The drains-source bias is set equal to 0.5V. (c) Absorption spectra of the two material. The band edge absorption of the HgTe QD is magnified 20 times to highlight the excitonic feature. Current as a function of the time under illumination by a laser at 405nm and 980nm under OV gate bias (d) and under 1.2V gate bias (e). (f) Evolution of the responsivity under light illumination at 405 and 980nm as a function of the gate bias.

CONCLUSION

We have demonstrated that electrolyte gating a CdSe/CdS NPL film using a solid electrolyte can significantly improve the photoresponse of the film by increasing its carrier lifetime. Improvement can be as high as 1000 and responsivity up to 50 $mA.W^{-1}$ have been achieved, which is the record for 2D colloidal CdSe nanoparticles. The electrolyte gating is also used as a switch to build a bicolor detector. The latter can respond to visible wavelength or to wavelength up to mid-IR depending on the applied gate bias. The method is general enough to be used for other colloidal semiconductor nanoparticles.

SUPPORTING INFORMATION

Additional material includes list of chemicals, nanoparticles synthesis and characterization, characteristic of ambipolar hybrid P3HT-CdSe/CdS NPL transistor.

AUTHORS IN FORMATIONS

EL and AR contributed equally to this work.

ACKNOWLEDGEMENTS

We thank Z. Xu for her help during the TEM imaging.

REFERENCES

1. Sargent, E. H. *Nat. Photonics* **2012,** 6, (3), 133-135.
2. Konstantatos, G.; Howard, I.; Fischer, A.; Hoogland, S.; Clifford, J.; Klem, E.; Levina, L.; Sargent, E. H. *Nature* **2006,** 442, (7099), 180-183.
3. Sukhovatkin, V.; Hinds, S.; Brzozowski, L.; Sargent, E. H. *Science* **2009,** 324, (5934), 1542-1544.
4. Keuleyan, S.; Lhuillier, E.; Brajuskovic, V.; Guyot-Sionnest, P. *Nat. Photonics* **2011,** 5, (8), 489-493.
5. Jeong, K. S.; Tang, J.; Liu, H.; Kim, J.; Schaefer, A. W.; Kemp, K.; Levina, L.; Wang, X. H.; Hoogland, S.; Debnath, R.; Brzozowski, L.; Sargent, E. H.; Asbury, J. B. *ACS Nano* **2012,** 6, (1), 89-99.
6. Rosencher, E.; Vinter, B., *Optoelectronic*. 2nd ed.; Dunod: Paris, 2002.
7. Lee, J. S.; Kovalenko, M. V.; Huang, J.; Chung, D. S.; Talapin, D. V. *Nat. Nanotechnol.* **2011,** 6, (6), 348-352.
8. Choi, J. H.; Fafarman, A. T.; Oh, S. J.; Ko, D. K.; Kim, D. K.; Diroll, B. T.; Muramoto, S.; Gillen, J. G.; Murray, C. B.; Kagan, C. R. *Nano Letters* **2012,** 12, (5), 2631-2638.
9. Ellingson, R. J.; Beard, M. C.; Johnson, J. C.; Yu, P. R.; Micic, O. I.; Nozik, A. J.; Shabaev, A.; Efros, A. L. *Nano Letters* **2005,** 5, (5), 865-871.
10. Luther, J. M.; Law, M.; Beard, M. C.; Song, Q.; Reese, M. O.; Ellingson, R. J.; Nozik, A. J. *Nano Letters* **2008,** 8, (10), 3488-3492.
11. Noh, Y. Y.; Kim, D. Y.; Yase, K. *J Appl Phys* **2005,** 98, (7), 7.
12. Yang, S. Y.; Zhao, N.; Zhang, L.; Zhong, H. Z.; Liu, R. B.; Zou, B. S. *Nanotechnology* **2012,** 23, (25), 6.
13. Nagpal, P.; Klimov, V. I. *Nat. Commun.* **2011,** 2, 7.
14. Hetsch, F.; Zhao, N.; Kershaw, S. V.; Rogach, A. L. *Mater. Today* **2013,** 16, (9), 312-325.
15. Lhuillier, E.; Aubin, H.; Ithurria, S.; Dubertret, B. *submitted* **2014**.
16. Talapin, D. V.; Lee, J. S.; Kovalenko, M. V.; Shevchenko, E. V. *Chem. Rev.* **2010,** 110, (1), 389-458.
17. Ithurria, S.; Dubertret, B. *J Am Chem Soc* **2008,** 130, (49), 16504-16505.
18. Ithurria, S.; Tessier, M. D.; Mahler, B.; Lobo, R. P.; Dubertret, B.; Efros, A. L. *Nat Mater* **2011,** 10, (12), 936-41.
19. Chen, Z.; Nadal, B.; Mahler, B.; Aubin, H.; Dubertret, B. *Adv. Funct. Mater.* **2013**.
20. Ithurria, S.; Talapin, D. V. *J Am Chem Soc* **2012,** 134, (45), 18585-90.
21. Nag, A.; Kovalenko, M. V.; Lee, J. S.; Liu, W. Y.; Spokoyny, B.; Talapin, D. V. *J Am Chem Soc* **2011,** 133, (27), 10612-10620.
22. Yu, D.; Wehrenberg, B. L.; Jha, P.; Ma, J.; Guyot-Sionnest, P. *J Appl Phys* **2006,** 99, (10).
23. Jarosz, M. V.; Porter, V. J.; Fisher, B. R.; Kastner, M. A.; Bawendi, M. G. *Phys Rev B* **2004,** 70, (19), 12.
24. Wang, C. J.; Shim, M.; Guyot-Sionnest, P. *Science* **2001,** 291, (5512), 2390-2392.
25. Sze, S. M.; Kwok, K., NG, *Physics of semiconductor devices*. wiley: 2007.
26. Lhuillier, E.; Keuleyan, S.; Liu, H.; Guyot-Sionnest, P. *Chem Mater* **2013,** 25, (8), 1272-1282.
27. Lhuillier, E.; Keuleyan, S.; Zolotavin, P.; Guyot-Sionnest, P. *Adv Mater* **2013**, (25), 137-141.
28. Lhuillier, E.; Keuleyan, S.; Rekemeyer, P.; Guyot-Sionnest, P. *J Appl Phys* **2011,** 110, (3), 8.